Forecasting Tornadic Thunderstorm Potential in Alberta Using Environmental Sounding Data. Part I: Wind Shear and Buoyancy

MAX L. DUPILKA AND GERHARD W. REUTER

University of Alberta, Edmonton, Alberta, Canada

(Manuscript received 17 December 2004, in final form 8 November 2005)

ABSTRACT

This study investigates, for Alberta, Canada, whether observed sounding parameters such as wind shear and buoyant energy can be used to help distinguish between thunderstorms with significant (F2–F5) tornadoes, thunderstorms with weak (F0–F1) tornadoes, and nontornadic severe thunderstorms. The observational dataset contains 87 severe convective storms, all of which occurred within 200 km of the upper-air site at Stony Plain, Alberta, Canada. Of these storms, 13 spawned significant (F2–F5) tornadoes, 61 spawned weak (F0–F1) tornadoes, and 13 had no reported tornadoes yet produced 3 cm or larger hailstones. The observations suggest that bulk shear contained information about the probability of tornado formation and the intensity of the tornado. Significant tornadic storms tended to have stronger shear values than weak tornadic or nontornadic severe storms. All significant tornado cases had a wind shear magnitude in the 900–500-mb layer exceeding 3 m s^{-1} km^{-1}. Combining the 900–500-mb shear with the 900–800-mb shear increased the probabilistic guidance for the likelihood of significant tornado occurrence. The data suggest that buoyant energy alone (quantified by the most unstable convective available potential energy) provided no skill in discriminating between tornadic and nontornadic severe storms, or between significant and weak tornadoes.

1. Introduction

During the summer months, severe convective storms with hail and, occasionally, tornadoes are often formed over Alberta, Canada (Smith and Yau 1993a,b; Smith et al. 1998; Hage 2003). Doppler radar observations are often used to provide watches or warnings for tornadic storms. A criterion for issuing a tornado watch is that the Doppler wind measurements indicate mesocyclone rotation. However, not all tornadoes are preceded by mesovortices, and not all supercells with mesovortices spawn tornadoes (Brooks et al. 1994a; Jones et al. 2004). The caveat of current Doppler-derived mesovortex algorithms is that they only indicate storm rotation once it has commenced. The short lead time for issuing and disseminating tornado watches offers little help for predicting the likelihood of tornado potential with lead times exceeding about 30 min.

To forecast the possibility of tornado potential several hours prior to the formation of thunderstorms, one can consider forecasting techniques based on prestorm sounding data, either from synoptic balloon soundings or from numerical weather prediction soundings at model grid points. Pioneering work in *The Thunderstorm Project* (Byers and Braham 1949) established the concept of a three-stage life cycle of a thunderstorm from initial cumulus development through storm maturity and eventual dissipation. Byers and Braham discussed the relation between wind shear and convective development. They noted that wind shear tends to retard the growth of nonprecipitating cumuli as the sheared flow displaces the center of maximum buoyancy relative to the core updraft. However, for precipitating storms with sufficiently strong updrafts, shear can enhance the circulation because the shear displaces precipitation out of the updraft, freeing it from the effects of precipitation drag. Fawbush et al. (1951) made early attempts at forecasting tornado potential by relating tornado events with observed soundings of temperature, dewpoint, and wind. Darkow and Fowler (1971) found that tornado environments were characterized by strong wind shear and veering of winds with height. Chisholm and Renick (1972) compared compos-

Corresponding author address: Dr. Gerhard Reuter, Dept. of Earth and Atmospheric Sciences, University of Alberta, Edmonton, AB T6G 2E3, Canada.
E-mail: gerhard.reuter@ualberta.ca

ite hodographs for different types of convective storms observed in Alberta. Weak wind shear was associated with short-lived airmass thunderstorms; while multicell storms tended to develop in strong unidirectional shear. Supercells were observed when there was strong directional shear in the lowest 2 km. Rasmussen and Wilhelmson (1983) found that tornadic storms tended to form in environments with high vertical wind shear and high convective available potential energy (CAPE), while nonrotating storms often formed in environments with low shear and low CAPE. Kerr and Darkow (1996) determined the relationship between environmental instability and tornadic intensity does not always hold. Bluestein and Jain (1985) constructed supercell mean profiles for storms in Oklahoma. McCaul (1991) notes these profiles approximate the findings of other composite tornado proximity studies (e.g., Maddox 1976; Schaefer and Livingston 1988).

Not all supercells produce tornadoes. It still remains uncertain whether tornadic storms develop in a shear environment markedly different from nontornadic severe thunderstorms and whether the intensity of tornadic storms is related to the amount of wind shear. However, there is evidence that the character of vertical wind shear, especially the near ground layer, does play a significant role in tornado development. Strong winds in the mid- to upper levels are suggested to be associated with significant tornadoes (Lemon andoswell 1979). Colquhoun and Shepherd (1989) examined the relationship between wind shear and tornado intensities. They found the magnitude of surface to 600-mb wind shear was correlated with tornado F-scale intensity. Brooks et al. (1994a) used numerical modeling to show the strength and persistence of low-level mesocyclones is influenced by the strength of the storm-relative midlevel flow environment. A study of cool season California storms indicated that environmental shear could be used as a discriminating factor between significant tornadic thunderstorms and severe thunderstorms that produced only weak tornadoes or no tornadoes at all (Monteverdi et al. 2003). Thompson et al. (2003) categorized three groups of severe storms as nontornadic, weakly tornadic (F0–F1), and significantly tornadic (F2 and greater). They found the 0–1-km vector shear magnitude showed discrimination between the significant tornadic and nontornadic events while the 0–6-km vector shear magnitude discriminated between supercells and nonsupercells but not between tornadic and nontornadic events.

The bulk Richardson number (BRN) is defined as BRN = CAPE/(½ U^2) (where U represents the difference between the density weighted mean winds in the 0–6-km and 0–500-m layers). As the BRN decreases, multicell convection becomes better organized, and at small enough values, quasi-steady supercell convection may occur. A storm environment with a high CAPE value and a BRN value less than about 50 increases the likelihood of a supercell storm, whereas a BRN larger than 50 tends to be associated with multicell storms (Weisman and Klemp 1982, 1986; Thompson et al. 2003). Rasmussen and Wilhelmson (1983) proposed that nonrotating thunderstorms could be found in environments of low shear and low CAPE while tornadic storms occurred with moderate to strong shear ($>3.5 \times 10^{-3}$ s^{-1}) and high CAPE (>2500 J kg^{-1}). However, the notion that high threshold values of shear and CAPE can readily discriminate between environments with severe and nonsevere thunderstorms may be an overgeneralization. Turcotte and Vigneux (1987) found that combined shear and CAPE criteria could not discriminate between tornadic and nontornadic severe storms. Brooks et al. (1994b) suggested this lack of discrimination is related to the theory that the occurrence of tornadoes is more closely associated with the development of low-level mesocyclones (i.e., below 1 km AGL), which are not characterized by CAPE. Brooks et al. (1994b) found that combinations of CAPE and shear did not discriminate between tornadic and nontornadic severe storms. Rasmussen and Blanchard (1998) showed some shear and CAPE combinations (such as the energy–helicity index) seemed useful in identifying environments that formed tornadic storms. However, they emphasized that the false alarm rate for these discriminators is still very high. Craven and Brooks (2004) introduced a strong tornado parameter (based on a combination of shear and CAPE) that showed separation between significant tornado and significant hail/wind events. Thompson et al. (2003) found marginal differences in CAPE between significant, weak, and nontornadic events. They also found that 0–1-km vector shear magnitude provided discrimination between the significant, weak, and nontornadic events, but 0–6-km shear vector magnitude did not. These and other studies (e.g., Kerr and Darkow 1996; Rasmussen and Blanchard 1998; Monteverdi et al. 2003) emphasize the important point that severe thunderstorm and tornadoes occur within a broad range of shear and CAPE environments. It is extremely important to keep in mind that it is likely the interaction of a number of physical processes that leads to tornadogenesis, and these processes may (or may not) be well represented by particular environmental parameters or variables we choose to examine (e.g., Rasmussen and Blanchard 1998). Even though, for example, the large-scale environment may contain enough deep layer shear, there may be insufficient low-level shear or

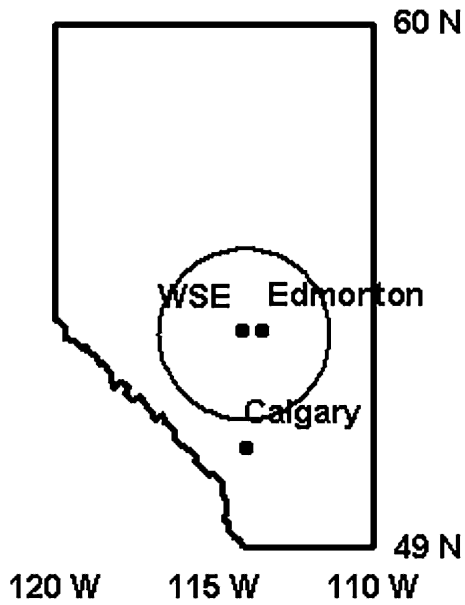

FIG. 1. Outline of AB showing the locations of the upper-air station at Stony Plain (WSE) and the cities of Edmonton and Calgary. The circle marks the 200-km radius from WSE.

buoyancy to develop a tornado. In addition there may be geographical differences in the storm environment and these differences should also be taken into account when assessing the importance of various sounding-derived parameters. Rasmussen (2003) showed that climatologically higher lifted condensation levels were associated with combined nonsignificant supercell plus significant tornadic storms for the Great Plains compared to regions farther east. Monteverdi et al. (2003) examined tornadic and nontornadic severe thunderstorms confined to California. Our research, which examines sounding-derived parameters, is also confined to a small region, being central Alberta.

This paper deals with forecasting the potential for tornadic development, given the existence of a severe thunderstorm, in the province of Alberta in Canada (Fig. 1). Smith et al. (1998) reported that, on average, Alberta has 51 days with hail each summer and 20 days with hailstones greater than 2 cm in diameter. Hage (2003) compiled an extensive tornado climatology covering the period 1879–1984. He reported that an average of about 10 tornadoes occur over Alberta each year, slightly less than Newark's (1984) estimate. Tornadic storms in central Alberta are generally associated with hail falling somewhere from the storm complex; yet less than 10% of Alberta hailstorms spawn tornadoes. Similar to other regions, tornadoes in Alberta are classified according to the Fujita damage scale (Fujita 1981) and most are rated at F0 or F1. However, most of the structural damage, injuries, and fatalities come from the more significant F2, F3, and F4 tornadoes. The motivation for our study is to investigate whether environmental sounding parameters, such as bulk shear, shear ratio, and buoyant energy, can be used to distinguish between tornadic and nontornadic severe storms in central Alberta. Furthermore, we want to explore whether sounding parameters can provide guidance to distinguish between significant (F2–F5) and weak (F0–F1) tornadoes. In Dupilka and Reuter (2006, Part II, appearing in this issue), we will focus on additional parameters, computed from the sounding data that may be related to tornadogenesis. Specifically, we will examine the role of storm-relative helicity, vortex spinup by storm convergence, and the amount of vertically integrated atmospheric water vapor (precipitable water).

2. Observations

The storm climatology dataset consists of 87 severe storm events occurring within 200 km of Stony Plain, Alberta (WSE), between 1967 and 2000 (Fig. 1). The data come from two sources. The storms prior to 1985 were taken from Hage's (2003) dataset, while those from 1985 and later were taken from the Severe Storm Archive of Environment Canada. Hage (2003) documented the date, location, and detailed type of damage of all recorded tornadoes occurring over Alberta based on newspaper reports, municipal records, insurance claims, and other archival data. He distinguished between tornadoes and other wind damage events such as downbursts. In this paper a "tornado event" is defined as a single tornado, not several spatially separate sightings of the same tornado. When accounts of a tornado occurred at separate locations within close proximity, this was assumed to be sightings of the same tornado and was taken to be a single event. When several reports of the same tornado occurred, the location with the greatest damage was used for the F-scale rating. All tornado events in Hage's Alberta tornado climatology (Hage 2003) that occurred prior to 1967 were eliminated because there were no soundings released in Alberta before 1967. Environment Canada's Severe Storms Archive was used to find tornado events for the period 1985–1997 plus the F3 Pine Lake tornado of 14 July 2000 (Erfani et al. 2002). In addition, we added 13 nontornadic severe storms from the Environment Canada dataset. All these nontornadic severe storms produced hail with sizes reported as 3 cm or larger. We refrained from using surface reports of damaging winds as an additional selection criterion for nontornadic severe storms because Environment Canada's Severe Storms Archive may not always distinguish between convective and nonconvective wind gusts.

Storm events were selected within a 200-km radius from the sounding site. Alberta has only one sounding site located at Stony Plain, WSE (53.5°N, 114.1°W, 766 m MSL). The 200-km threshold radius captured most of the significant tornado events (≥F2) while still maintaining a reasonable spatial proximity. The Hage dataset does not record the exact time of day for tornado occurrence; therefore, the 0000 UTC (1800 local daylight time) sounding corresponding to the day of the tornado event was chosen. Most Alberta thunderstorms occur in the late afternoon or evening (Newark 1984). From the Environment Canada dataset the mean time for storms with hail sizes of 1 cm or greater is about 2350 UTC with roughly 93% occurring within ±6 h of 0000 UTC. Therefore, we feel the choice of 0000 UTC sounding was reasonably representative of the temporal diagnostic storm environment in question. All storms after 1984 occurred with a time window within ±6 h of 0000 UTC. Smaller spatial and temporal constraints may provide better proximity soundings, but at the expense of a smaller dataset. To ensure the soundings were most likely to represent the storm environment, we implemented additional quality controls. Each sounding was manually inspected using raob for Windows software from Environmental Research Services (Shewchuk 2002). Soundings were rejected if the most unstable CAPE (Doswell and Rasmussen 1994) was less than 50 J kg^{-1}. This eliminated soundings more indicative of dry microbursts, dry dust devils, and saturated profiles that may indicate the sounding ascended through a thunderstorm. Soundings suspected of indicating frontal passages were checked against the previous 1200 UTC sounding and rejected if a frontal passage appeared likely. These restrictions resulted in 74 tornado and 13 nontornado severe thunderstorm events in our dataset while eliminating 30 tornado cases and 1 nontornado case. The choices of spatial and temporal soundings emphasize the difficulties associated with obtaining a sufficiently large dataset for rare events.

The frequency of tornado occurrence versus F-scale values for our dataset is shown in Fig. 2. The F0 tornado events dominate (49 cases) out of the total 74 cases. There were 12 F1 tornadoes, 6 F2 tornadoes, and 6 F3 tornadoes. The F3 Holden tornado of 29 July 1993 and the F3 Pine Lake tornado of 14 July 2000 were analyzed by Dupilka and Reuter (2004). There was only one F4 tornado, the Edmonton F4 tornado of 31 July 1987 (Dupilka and Reuter 2004). There has not been an F5 tornado reported in Alberta. Shown for comparison (Fig. 2, solid line) is the frequency of F-scale tornadoes in Canada during the period 1958–98 (Brooks and Doswell 2001; Dotzek et al. 2003). Approximately 23% of Canadian tornadoes occur in Alberta. The frequency distribution of the Alberta tornado events is similar to that of the entire Canadian tornado events dataset.

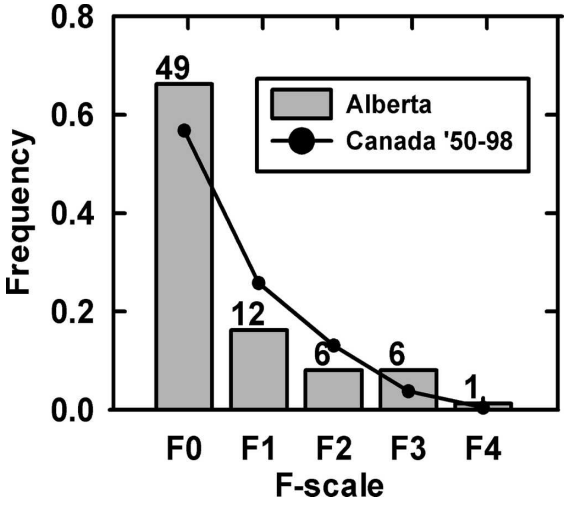

FIG. 2. Frequency of tornadoes in F-scale categories. The bars show the frequency for the study cases in central AB during the period from 1967 to 2000. The total number of cases is 74. The value above each bar indicates the number of study cases in that F group. The dots and line show the frequency of events in Canada during the period from 1950 to 1998.

Following the study of Thompson et al. (2003), we categorized the tornadic events into two separate classes: significant tornado (ST) events that consisted of F2, F3, and F4 tornadoes, and weak tornado (WT) events that consisted of F0 and F1 tornadoes. With these two categories the Alberta dataset divided into 18% ST cases and 82% WT cases. The ratios of the entire Canadian dataset were identical: 18% ST and 82% WT.

3. Calculation of sounding parameters

Environmental Research Services has developed an extensive software package (raob) to display and analyze sounding data. The raob software was used to compute sounding parameters for WSE soundings data. Sounding data were obtained from a CD-ROM, *Rawindsonde Data of North America 1946–1992,* and through an online database (post-1992) produced jointly by the National Climate Data Center (NCDC) and the Forecast Systems Laboratory (FSL). The sounding data are available online (http://raob.fsl.noaa.gov). Since the wind measurements were archived at fixed pressure levels, bulk shear (SHR) was computed using

$$\mathrm{SHR} = \frac{\sqrt{(u_2 - u_1)^2 + (v_2 - v_1)^2}}{|z_2 - z_1|}, \qquad (1)$$

where (u_x, v_x) denote the zonal and meridional components of the wind vector and z_x denotes the height at pressure level p_x. We computed bulk shear in the layers from 900 to 800 (SHR8), 900 to 700 (SHR7), 900 to 600 (SHR6), and 900 to 500 mb (SHR5). The terrain of Alberta varies significantly, ranging from mountainous in the west to flatland in the east with numerous valleys and hills in between. The surface pressure values of the storm environment range from about 940 to 900 mb. The wind measurements sampled from surface observation sites indicate significant temporal and spatial variability, which tends to be affected by the differential heating of the uneven terrain. To reduce surface complexities we computed bulk shear values using the 900-mb wind from the sounding rather than the surface-based wind observation. In previous studies wind shear was often computed for specified altitudes instead of pressure levels (e.g., Brooks et al. 1994b; Thompson et al. 2003). The reason for sticking to pressure levels is because these are commonly used by Alberta forecasters. Most unstable CAPE (MUCAPE) is computed using the virtual temperature of the most unstable parcel in the lowest 300 mb (Doswell and Rasmussen 1994). MUCAPE values are sensitive to the temperature and humidity sounding. Since spatial and temporal variability in temperature and humidity can dominate in the lower levels, MUCAPE values derived from proximity soundings may not always be representative of the local storm environment.

4. Environmental wind shear

a. Bulk shear

Our focus is on finding the correlation between observed shear with the occurrence of significant tornado (ST) events, weak tornado (WT) events, and nontornadic severe hail (NT) events. Figure 3 shows box and whisker plots for bulk shear (SHR8, SHR7, SHR6, and SHR5) values. The horizontal bar indicates the median value; the gray boxes denote the 25th–75th percentiles (the so-called 50% boxes), and the whiskers show the full range of shear values. For the 900–800-mb shear the median for the NT case was 5.0 m s^{-1} km^{-1}, for the WT case it was lowest at 4.1 m s^{-1} km^{-1}, while the ST case was greatest at 7.4 m s^{-1} km^{-1}. For the 900–500-mb shear the median for the NT case was 3.4 m s^{-1} km^{-1}, for the WT case it was again lowest at 2.2 m s^{-1} km^{-1}, and the ST case was largest at 5.0 m s^{-1} km^{-1}. For all four layers shown, the median shear values for ST cases were larger than for WT or NT cases. A similar finding is apparent in the 50% gray boxes. The 50% boxes of shear values for the ST events showed little overlap with the WT cases and generally small overlap with the NT cases. For instance, in the 900–500-mb layer, the 25th percentile for the ST (4.3 m s^{-1} km^{-1}) cases is separated from the 75th percentile for WT cases (3.8 m s^{-1} km^{-1}) and only slightly overlaps the NT 50% box (75th percentile of 4.8 m s^{-1} km^{-1}). For all four layers, the WT 50% boxes were consistently lowest. The NT 50% boxes were slightly higher than the WT cases but, generally, with a large overlap between these two events.

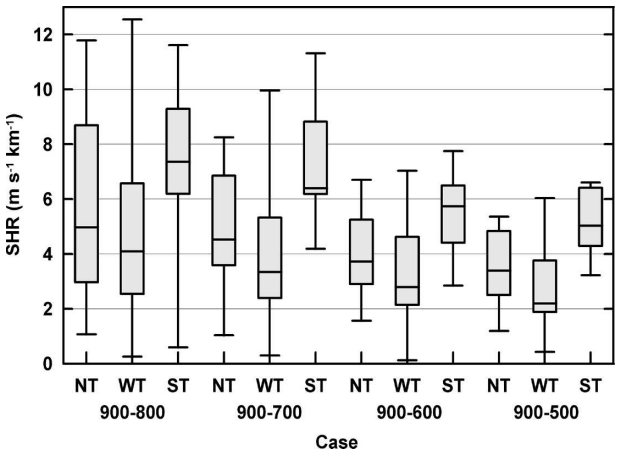

FIG. 3. Box and whiskers plots of SHR values for nontornado (NT) and tornado (WT, ST) cases in the layers at 900–800, 900–700, 900–600, and 900–500 mb. Gray boxes denote the 25th–75th percentiles, with a heavy solid horizontal bar at the median value. The vertical lines (whiskers) extend to the maximum and minimum values.

To determine whether the shear differences between the storm categories within each layer were statistically significant we performed Mann–Whitney (e.g., Miller et al. 1990) tests for the SHR8, SHR7, SHR6, and SHR5 values for pairings of the ST, WT, and NT events. The Mann–Whitney test is a nonparametric rank-randomization two-sample test. Whereas the popular Student's *t* test has the inherent assumption that values have a normal bell-shaped distribution, the Mann–Whitney test has no such constraint. The test ranks all of the values from two groups together from lowest to highest, and compares the mean values of the ranking of the two groups. The result is a confidence probability for the question: "If the means of the two groups are the same, what is the chance that random sampling would result in sample means being as far apart as observed in the test?" The Student's *t* test requires samples sizes of 30 or more while the Mann–Whitney test provides statistically reliable results when both sample sizes are greater than 8 (Miller et al. 1990, 198, 308). The Mann–Whitney test for the SHR8 and SHR5 parameters found statistically significant differences at the 1% level between the ST and WT events.

Statistically significant differences at the 3%–5% level were found for NT–WT pairs based on SHR5, and also NT–ST pairs based on SHR7. There were no significant differences between NT–WT pairs based on SHR8, SHR7, and SHR6 shears. Overall, SHR5 showed statistically significant differences at the 5% or less level between all three categories. This suggests that the bulk shear for the 900–500-mb layer provides the best assistance in discriminating between ST, WT, and NT cases, although there appears to be useful discrimination information contained in all shear layers.

It has been suggested that tornadogenesis is closely connected to the formation of a low-level mesocyclone (e.g., Thompson et al. 2003). Therefore, the shear in the 900–800-mb layer (SHR8) may be associated with the production of low-level mesocyclones through tilting of horizontal vorticity into the vertical within the inflow region of the updraft. Since SHR8 showed significant differences between the WT and ST cases, it may also be a useful parameter for distinguishing between weak and significant tornado formations.

b. Bulk shear ratio

Reuter and Jacobsen (1993) drew attention to the fact that convection is not only affected by the amount of the bulk shear, but also to the ratio of low-level shear to the total shear. They reported the following findings based on slab-symmetric modeling. When the wind profile indicates a concave bulge (i.e., low-level shear is larger than the deep-layer shear), the updraft–downdraft circulation becomes stronger and more organized in comparison with the linear wind profile. Conversely, the circulation becomes weaker when the wind profile had a convex shape. For a fixed gross shear magnitude, increasing the concave bulge tends to intensify the circulation. Thus, the detail of the wind profile can affect the convective storm intensity. Based on the findings by Reuter and Jacobsen, we were interested to determine whether the ratio of shears β, defined as

$$\beta \equiv \frac{\text{SHR8}}{\text{SHR5}}, \tag{2}$$

could provide information about the likelihood of tornado potential. The box and whisker plot (Fig. 4) compares the β values for NT, WT, and ST events. The data suggest that the β value did not help distinguish between the three groups. The 25th–75th percentile range for all cases was similar. The widest overall range occurred for the WT cases ($0.2 \leq \beta \leq 6.8$), the smallest range was for ST values ($0.1 \leq \beta \leq 3.6$). The median values showed a very slight increase from NT (1.3) to WT (1.5) to ST (1.7). The small variation in the 50% boxes of all events suggests that the low-level shears were strongly coupled with the deep-layer shears. The frequency distribution of β values for the combined set of all NT, WT, and ST events (Fig. 5) indicates the narrow range of distribution for a large percentage of β values ($1 \leq \beta \leq 2.$). The maximum frequency of 0.17 occurs for $\beta = 1.4$.

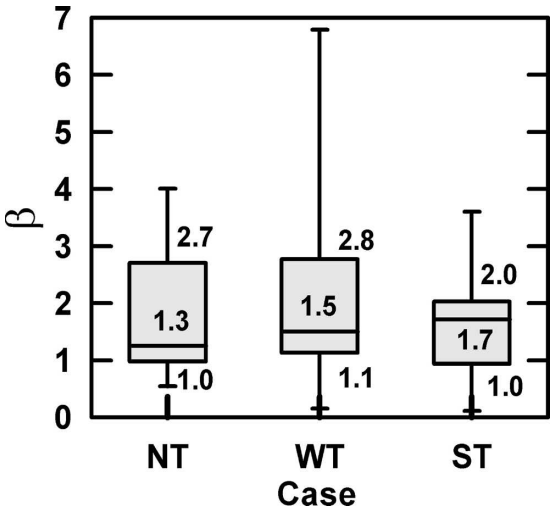

FIG. 4. Box and whisker plots of β = SHR8/SHR5 for NT, and WT and ST cases.

The Alberta storm data suggest that ST events tended to have strong wind shear in the deep layer from 900 to 500 mb. Mann–Whitney statistics showed the

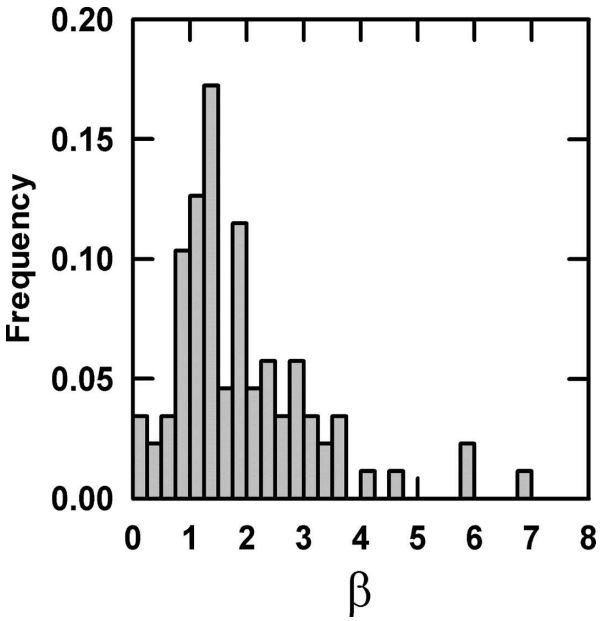

FIG. 5. Frequency of occurrence of β for the combined set of cases in the study (NT, WT, and ST).

SHR5 values appeared to provide the best discrimination between severe thunderstorms that could potentially produce F2–F4 tornadoes from those that likely produced either F0–F1 tornadoes or no tornadoes at all. The low-level shear (900–800 mb) could also distinguish significant from weak tornadoes. These findings add support to the hypothesis put forth by Johns and Doswell (1992) that severe storms may form tornadoes when low-level shear in the buoyant inflow layer is coupled with deep-layer shear to generate a mesocyclone. Johns and Doswell state that, in general, strong to violent supercell tornado events observed in lower-buoyancy environments are associated with stronger low-level shear values than those observed with higher-buoyancy cases. Later work has shown that tornadoes can develop in environments of both low CAPE and low environmental wind speed (e.g., Kerr and Darkow 1996). This implies that different combinations of buoyancy and shear values could result in tornado development. For example, in low-buoyancy environments, where the amount of deep-layer shear is sufficient for the formation of supercells, the low-level shear may augment the updraft enough to promote tornadic development. Observed and modeling results (e.g., Weisman and Klemp 1982; Thompson et al. 2003) have indicated that thunderstorms growing in environments of 0–6-km shear of 3–5 m s^{-1} km^{-1} show a slight tendency for organization into supercells, whereas those growing in environments of 0–6-km shear > 5 m s^{-1} km^{-1} have a slight tendency to become stronger and more persistent supercells. Our results show that NT and ST storms had SHR5 shear values in the 25th–75th percentile that were generally greater than 3 m s^{-1} km^{-1}, similar to values for supercell formation. The weaker F0–F1 storms tended to have lower shear values, possibly suggesting that these tornadoes were not all spawned by supercell thunderstorms.

c. Directional shear

As discussed in the introduction, the development and maintenance of supercells and possible tornado formation can be influenced by veering of the wind in the low levels. To quantify the wind speed and amount of veering, we examined an INIS parameter introduced by Colquhoun and Shepherd (1989), which accounts for both speed and directional shear. INIS is proportional to the length of a hodograph between two pressure levels (see Fig. 2 in Colquhoun and Shepherd 1989):

$$\text{INIS} \equiv \frac{\left|\sum[\text{IN(L)} \cdot \Delta p]\right| + \left|\sum[\text{IS(L)} \cdot \Delta p]\right|}{\sum \Delta p \sum |\Delta z|}, \quad (3)$$

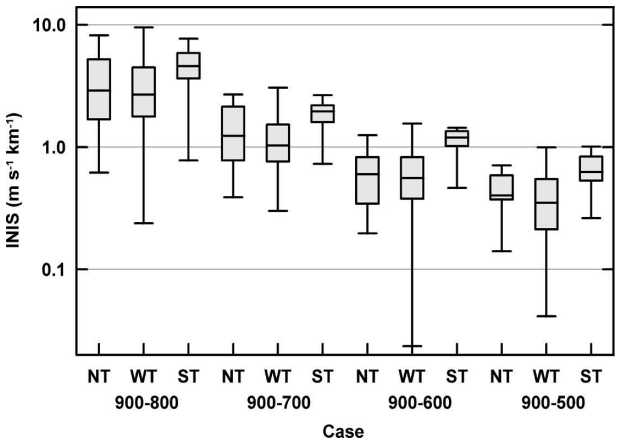

FIG. 6. Box and whiskers plots of INIS values for NT, and WT and ST cases in the layers at 900–800, 900–700, 900–600, and 900–500 mb.

where IN(L) $= |\mathbf{V}_p| \sin\theta$ and IS(L) $= |\mathbf{V}_p| \cos\theta - |\mathbf{V}_{p+\Delta p}|$. Here, θ is the angle between wind vectors $\mathbf{V}_p$ and $\mathbf{V}_{p+\Delta p}$ at pressures p and $p + \Delta p$; IN(L) and IS(L) are, respectively, the components of the wind shear in a given layer L, normal to and in the direction of the wind at the base of the layer; IN(L) relates to the directional shear and IS(L) to the speed shear. The INIS values were calculated between pressure levels p and $p + \Delta p$ where $\Delta p = 50$-mb increments and Δz was the height difference between pressure levels.

Similar to bulk shear, we calculated INIS values in the layers 900–800, 900–700, 900–600, and 900–500 mb. Box and whisker plots for INIS shear values are shown for the three storm categories (Fig. 6). As with the SHR bulk shear values, the middle 50% of the INIS shear values of the four layers for the ST cases generally showed significant separation from the WT and NT cases, while there was a large overlap between WT and NT cases. The ST cases distinctly had the greatest medians values: the median values for the 900–500-mb layer range from 0.40 (NT) to 0.35 (WT) to 0.63 (ST); for the 900–800-mb layer the median values are 2.91 (NT), 2.69 (WT), and 4.60 (ST). Mann–Whitney tests for paired cases of INIS values within each layer confirmed that the ST cases had statistically significant differences in values (at the 1% or less level) from the NT and WT cases. However, other paired cases generally did not show differences at the 5% level. Overall, INIS values provided slightly less separation of the three cases than SHR bulk shears. Since bulk shear is conceptually a more direct parameter, while offering better discrimination for our dataset, it may be more useful for the operational forecaster than INIS shear for assessing tornadic potential.

5. Most unstable convective available energy and bulk Richardson number

Studies (e.g., Brooks et al. 1994b; Thompson et al. 2003) have found that the amount of buoyant energy by itself offered no useful assistance in discriminating between tornadic and nontornadic severe storms. We turn our attention to the use of most unstable convective available potential energy (MUCAPE) to determine whether total buoyant energy can distinguish between NT, WT, and ST events occurring in Alberta. Figure 7 compares the box and whisker plots for the three storm groups. The ST and NT events had similar median MUCAPE values of about 1050 J kg^{-1} while the WT events had the lowest median value (~900 J kg^{-1}). The WT events showed the widest overall range of MUCAPE values, consistent with the fact that this group contained the most storms. There is no trend toward increasing MUCAPE values being associated with NT through ST storms. The Mann–Whitney tests indicated there were no statistically significant differences for the MUCAPE values between the NT, WT, and ST groups. This suggests that MUCAPE alone offers little help in predicting the likelihood of tornado formation or in predicting the likely intensity of the tornado should it form. We also calculated the mean parcel CAPE (MLCAPE) using the lowest 100 mb as the mixed layer (Craven et al. 2002). We found MLCAPE gave a similar distribution to the MUCAPE values; there were no significant differences between the NT, WT, and ST groups.

We next examined a modified form of the bulk Richardson number (BRN) to determine if it was useful for discriminating between the three storm types (ST, WT, and NT). Values of BRN were calculated using MUCAPE and 900–500-mb shear (rather than the traditional shear between the 0–0.5-km layer and the 0–6-km density-weighted mean wind). Figure 8 shows BRN values indicated some discrimination of the ST events from the WT and NT groups. The median values for the NT, WT, and ST cases are 9, 14, and 4, respectively. A Mann–Whitney test confirmed the ST cases showed a difference from the WT cases that is statistically significant at the 5% level. There were no statistically significant differences between the other combinations of cases. Therefore, BRN offers less guidance than shear, but more than MUCAPE. Results showed BRN values of all groups up to the 75th percentile fell below ~50, suggesting that many events might have been associated with supercell storms.

6. Assessing the risk for significant tornadoes

The Alberta data suggest that SHR8 and SHR5 values provide information concerning the conditional likelihood of tornado formation given the occurrence of a severe storm. The scatterplot of SHR5 and SHR8 values (Fig. 9) suggests that a pair of SHR5 and SHR8 threshold values might be more useful than either shear parameter threshold alone in distinguishing between ST and WT cases. For each threshold pair (SHR5*–SHR8*) we can associate the (quadrant) parameters space (SHR5 ≥ SHR5*, SHR8 ≥ SHR8*). Figure 9 shows two specific cases of threshold pairs. Using the threshold pair (SHR5* = 3 m s^{-1} km^{-1}, SHR8* = 6 m s^{-1} km^{-1}) 77% of all ST events occurred within this

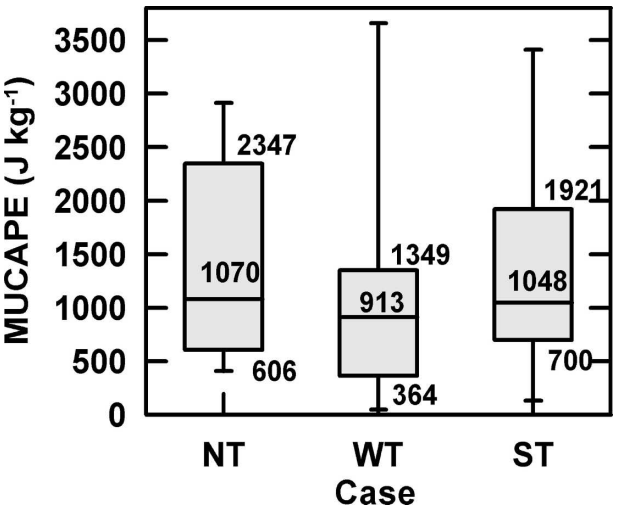

FIG. 7. Box and whiskers plots of MUCAPE for NT, WT, and ST cases.

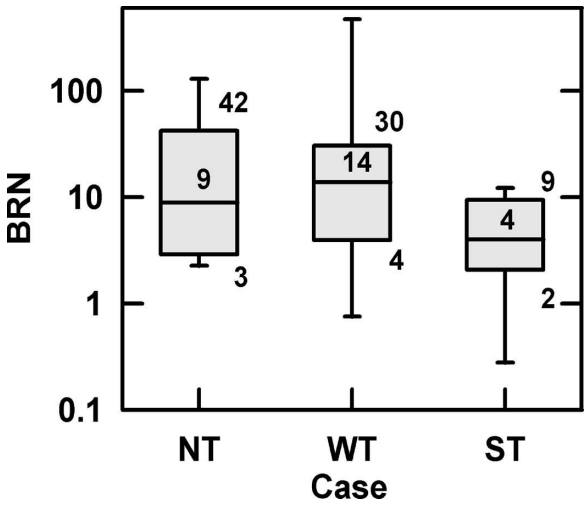

FIG. 8. Box and whiskers plots of BRN for NT, WT, and ST cases.

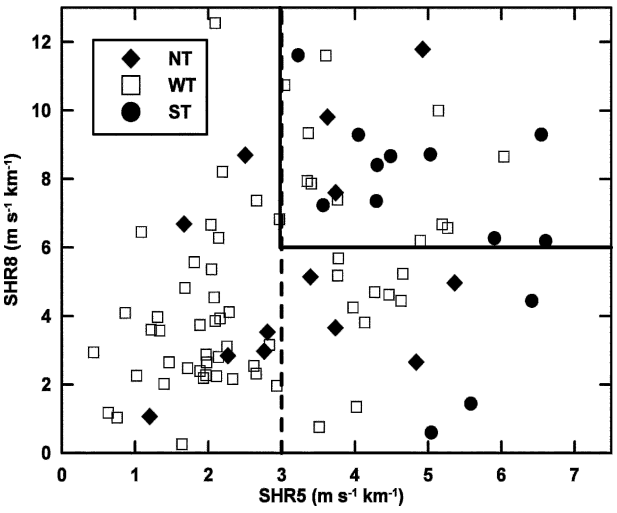

FIG. 9. Scatterplot of SHR8 vs SHR5 for the 87 Alberta storms categorized into NT (diamonds), WT (squares), and ST (dots) cases. The solid (dashed) line marks the 77% (100%) threshold for ST events.

parameter space whereas only 18% of the WT events were contained here (solid box in Fig. 9; see Table 1). Also, only 23% of the NT cases occurred here. This suggests that the threshold pair (SHR5* = 3 m s^{-1} km^{-1}, SHR8* = 6 m s^{-1} km^{-1}) offers some skill in providing probabilistic guidance about the conditional likelihood of significant tornadoes versus nonsignificant tornadoes. Specifically, it was found that only 23% of all ST events had SHR5 and SHR8 values that lay outside of the quadrant (SHR5 $\geq$ 3 m s^{-1} km^{-1}, SHR8 $\geq$ 6 m s^{-1} km^{-1}). If we lower the threshold values for the shear values, we increase the size of the quadrant, and this is associated with an increased frequency percentage of ST events. So essentially we can increase the "probability of detection" of ST events; however, this also results in an associated increase in the "false alarm rate" of ST events. Suppose we keep the threshold SHR5* = 3 m s^{-1} km^{-1}, but decrease the SHR8* threshold from 6 to 4 m s^{-1} km^{-1}. Table 1 shows that the frequency percentage values for ST events increases from 77% to 85%, yet at the same time the percentage frequencies for WT and NT events are increased to 30% (from 18%) and 38% (from 23%), respectively. To capture all ST events, one could relax the SHR8* threshold to 0 m s^{-1} km^{-1} (indicated as the dashed line in Fig. 9). This suggests that *all historic* ST cases for Alberta had a 900–500-mb shear exceeding 3 m s^{-1} km^{-1}; yet there were many cases of WT events and NT events that had shears also exceeding that threshold. Increasing the SHR8* threshold to 8 m s^{-1} km^{-1} lowers the percentage frequency of ST events to 46% but improves the false alarm rate as there were only 8% of WT and NT cases included in this parameter space. It may be unwise to place too much emphasis on an inferred false alarm rate. Rasmussen and Blanchard (1998) point out that even for relatively strong discriminators their false alarm rate was very high. This could likely be generalized to our results as well.

TABLE 1. Percent occurrence of ST, WT, and NT events for 900–800- and 900–500-mb (SHR8*–SHR5*) shear threshold pairs. Shear is in m s^{-1} km^{-1}.

Shear thresholds		Percent occurrence		
SHR5*	SHR8*	ST	WT	NT
3.0	8.0	46	8	8
3.0	6.0	77	18	23
3.0	4.0	85	30	38
3.0	0.0	100	34	54

From the preceding discussions it is apparent that a forecaster should decide upon an "acceptable" probability of occurrence of ST events, while still maintaining a sufficiently low-frequency percentage of WT or NT events. In some cases, the risks of missing a significant event may be so crucial that it is better to "overforecast" the likely occurrence of significant tornadoes. In other situations it may be more prudent to lower the percentage of "false alarms," while allowing for more tolerance of missing a significant event. This probabilistic nature of the risk assessment has been discussed in more detail by Brooks (2004).

7. Conclusions and discussion

We investigated the usefulness of selected sounding parameters for discriminating between ST, WT, and NT events. Bulk shear within the 900–500-mb layer (SHR5) showed statistically significant differences for values between the NT, WT, and ST events. The low-level shear in the 900–800-mb layer (SHR8) also showed skill in discriminating ST events from WT events. These differences suggest that shear threshold pairs (SHR5*–SHR8*) might help to assess the potential for thunderstorms to become tornadic. Also, the thresholds could be useful for separating significant tornadoes from weak tornadoes. The Alberta data suggest that the threshold pair of (SHR5* = 3 m s^{-1} km^{-1}, SHR8* = 6 m s^{-1} km^{-1}) would have captured roughly about 75% of the ST cases. To use these thresholds, a forecaster would have to decide if the corresponding percentage of false alarms is acceptable. Lowering the number of false alarm values is, however, associated with a corresponding lowering of the probability of detection of

these significant events (Brooks 2004). It is interesting to note the F4 Edmonton tornado of 31 July 1987 (Dupilka and Reuter 2004) had SHR5 and SHR8 values of 6.5 and 9.3 m s^{-1} km^{-1}, respectively, well within the parameter space defined by the thresholds in Table 1.

A large portion of the 900–500-mb shear values for NT and ST storms were greater than 3 m s^{-1} km^{-1}, similar to the 3–5 m s^{-1} km^{-1} values associated with supercell formation found by other authors (e.g., Weisman and Klemp 1982; Thompson et al. 2003). The weaker WT storms tended to have lower shear values, which may suggest that not all of these storms were associated with supercell thunderstorms. The ratio of shears, β (=SHR8/SHR5), did not show any statistically significant differences between any of the three storm groups (NT, WT, ST). The greatest frequency of β values occurred between about 1 and 2. The Edmonton tornado, discussed previously, had $\beta = 1.4$, which corresponded to the maximum frequency of β for our tornado dataset (Fig. 5).

We found that buoyant energy alone could not distinguish between the three categories of events. A modified form of the BRN showed limited skill in distinguishing between WT and ST events, related to the finding that buoyant energy was not well correlated with different storm categories.

It is important to realize the shortcomings and complications inherent to our empirical study. A major issue is to what extent the observed sounding data released from WSE at 0000 UTC are indeed representative for the air mass that feeds the severe storms. Brooks et al.(1994b) and Monteverdi et al. (2003) discussed the complexities associated with observed proximity soundings. Parameters such as MUCAPE can be very sensitive to low-level changes in temperature and dewpoint. Numerical cloud modeling by Brooks et al. (1994a) showed the effects of convection can cause changes in these parameters on space and time scales comparable to the development of thunderstorms. Markowski et al. (1998) concluded that major variations in thermodynamic parameters can occur over time and space scales comparable to the duration of thunderstorm development. In contrast, Markowski et al. (1998) noted that 0.5–6-km wind shear was fairly uniform over large distances. A study of storm motion by Bunkers (2002) also suggests shear parameters derived from proximity soundings could be more robust and less sensitive to local variations compared to other parameters such as MUCAPE. Our study is also limited by the relatively small number of significant tornado events. These cases are rare and are coupled with the sparseness of upper-air stations in Alberta. The problem of sounding scarcity in Alberta is not likely to change in the foreseeable future. Numerical model sounding data may help obtain a larger dataset and also allow for smaller proximity ranges. Future work should include expanding the dataset and investigating the use of numerical model soundings to better simulate local storm environments.

In conclusion, we would like to stress that there does not exist a *complete* understanding of the processes of tornadogenesis, and that our findings should be used as *guidelines*. Our results on shear threshold values should be considered in a probabilistic manner. That is, within the parameter space there are regions where, given the development of a severe thunderstorm, the probability of that thunderstorm becoming tornadic is greater than in other areas. Additionally, there are regions in the parameter space where a given thunderstorm has a greater potential to develop into a significant tornado.

Acknowledgments. This research is supported by the Canadian Foundation for Climate and Atmospheric Sciences (CFCAS). This work would not have been possible without the careful and detailed work by Dr. Keith Hage in assembling a climatology of Alberta tornadoes. The authors are appreciative for the comments and constructive criticisms of the anonymous reviewers.

REFERENCES

Bluestein, H. B., and M. H. Jain, 1985: Formation of mesoscale lines of precipitation: Severe squall lines in Oklahoma during the spring. *J. Atmos. Sci.,* **42,** 1711–1732.

Brooks, H. E., 2004: Tornado-warning performance in the past and future: A perspective from signal detection theory. *Bull. Amer. Meteor. Soc.,* **85,** 837–843.

——, and C. A. Doswell III, 2001: Some aspects of the international climatology of tornadoes by damage classification. *Atmos. Res.,* **56,** 191–202.

——, ——, and R. B. Wilhelmson, 1994a: The role of midtropospheric winds in the evolution and maintenance of low-level mesocyclones. *Mon. Wea. Rev.,* **122,** 126–136.

——, ——, and J. Cooper, 1994b: On the environment of tornadic and nontornadic mesocyclones. *Wea. Forecasting,* **9,** 606–618.

Bunkers, M. J., 2002: Vertical wind shear associated with left-moving supercells. *Wea. Forecasting,* **17,** 845–855.

Byers, H. R., and R. R. Braham Jr., 1949: *The Thunderstorm.* U.S. Government Printing Office, 287 pp.

Chisholm, A. J., and J. H. Renick, 1972: The kinematics of multicell and supercell Alberta hailstorms. Research Council of Alberta Hail Studies Rep. 72-2, 7 pp.

Colquhoun, J. R., and D. J. Shepherd, 1989: An objective basis for forecasting tornado intensity. *Wea. Forecasting,* **4,** 35–50.

Craven, J. P., and H. E. Brooks, 2004: Baseline climatology of sounding derived parameters associated with deep moist convection. *Natl. Wea. Dig.,* **28,** 13–24.

——, R. E. Jewell, and H. E. Brooks, 2002: Comparison between observed cloud-based heights and lifting condensation level for two different lifted parcels. *Wea. Forecasting,* **17,** 885–890.

Darkow, G. L., and M. G. Fowler, 1971: Tornado proximity wind sounding analysis. Preprints, *Seventh Conf. on Severe Local Storms,* Kansas City, MO, Amer. Meteor. Soc., 148–151.

Doswell, C. A., III, and E. N. Rasmussen, 1994: The effect of neglecting the virtual temperature correction on CAPE calculations. *Wea. Forecasting,* **9,** 625–629.

Dotzek, N., J. Grieser, and H. E. Brooks, 2003: Statistical modeling of tornado intensity distributions. *Atmos. Res.,* **67–68,** 163–187.

Dupilka, M. L., and G. W. Reuter, 2004: A case study of three severe tornadic storms in Alberta, Canada. Preprints, *22d Conf. on Severe Local Storms,* Hyannis, MA, Amer. Meteor. Soc., CD-ROM, 3A.6.

——, and ——, 2006: Forecasting tornadic thunderstorm potential in Alberta using environmental sounding data. Part II: Helicity, precipitable water, and storm convergence. *Wea. Forecasting,* **21,** 336–346.

Erfani, A., A. Methot, R. Goodson, S. Belair, K. S. Yeh, J. Cote, and R. Moffet, 2002: Synoptic and mesoscale study of a severe convective outbreak with the nonhydrostatic Global Environmental Multiscale (GEM) model. *Meteor. Atmos. Phys.,* **82,** 31–53.

Fawbush, E. J., R. C. Miller, and L. G. Starrett, 1951: An empirical method of forecasting tornado development. *Bull. Amer. Meteor. Soc.,* **32,** 1–9.

Fujita, T. T., 1981: Tornadoes and downbursts in the context of generalized planetary scales. *J. Atmos. Sci.,* **38,** 1511–1534.

Hage, K. D., 2003: On destructive Canadian prairie windstorms and severe winters. *Nat. Hazards,* **29,** 207–228.

Johns, R. H., and C. A. Doswell III, 1992: Severe local storms forecasting. *Wea. Forecasting,* **7,** 588–612.

Jones, T. A., K. M. McGrath, and J. T. Snow, 2004: Association between NSSL Mesocyclone Detection Algorithm–detected vortices and tornadoes. *Wea. Forecasting,* **19,** 872–890.

Kerr, B. W., and G. L. Darkow, 1996: Storm-relative winds and helicity in the tornadic thunderstorm environment. *Wea. Forecasting,* **11,** 489–505.

Lemon, L. R., and C. A. Doswell III, 1979: Severe thunderstorm evolution and mesocyclone structure as related to tornadogenesis. *Mon. Wea. Rev.,* **107,** 1184–1197.

Maddox, R. A., 1976: An evaluation of tornado proximity wind and stability data. *Mon. Wea. Rev.,* **104,** 133–142.

Markowski, P. M., J. M. Straka, E. N. Rasmussen, and D. O. Blanchard, 1998: Variability of storm-relative helicity during VORTEX. *Mon. Wea. Rev.,* **126,** 2959–2971.

McCaul, E. W., Jr., 1991: Bouyancy and shear characteristics of hurricane–tornado environments. *Mon. Wea. Rev.,* **119,** 1954–1978.

Miller, I., J. E. Freund, and R. A. Johnson, 1990: *Probability and Statistics for Engineers*. 4th ed. Prentice Hall, 612 pp.

Monteverdi, J. P., C. A. Doswell III, and G. S. Lipari, 2003: Shear parameter thresholds for forecasting tornadic thunderstorms in northern and central California. *Wea. Forecasting,* **18,** 357–370.

Newark, M. J., 1984: Canadian tornadoes, 1950–1979. *Atmos.–Ocean,* **22,** 343–353.

Rasmussen, E. N., 2003: Refined supercell and tornado forecast parameters. *Wea. Forecasting,* **18,** 530–535.

——, and R. B. Wilhelmson, 1983: Relationships between storm characteristics and 1200 GMT hodographs, low level shear and stability. Preprints, *13th Conf. on Severe Local Storms,* Tulsa, OK, Amer. Meteor. Soc., 55–58.

——, and D. O. Blanchard, 1998: A baseline climatology of sounding-derived supercell and tornado forecast parameters. *Wea. Forecasting,* **13,** 1148–1164.

Reuter, G. W., and O. Jacobsen, 1993: Effects of variable wind shear on the mesoscale circulation forced by slab-symmetric diabatic heating. *Atmos.–Ocean,* **31,** 451–469.

Schaefer, J. T., and R. L. Livingston, 1988: The typical structure of tornado proximity soundings. *J. Geophys. Res.,* **93,** 5351–5364.

Shewchuk, J., 2002: RAOB (the Rawinsonde Observation Program) for Windows. Version 5.1, Environmental Research Services. [Available from Environmental Research Services, 1134 Delaware Dr., Matamoras, PA 18336.].

Smith, S. B., and M. K. Yau, 1993a: The causes of severe convective outbreaks in Alberta. Part I: A comparison of a severe outbreak with two nonsevere events. *Mon. Wea. Rev.,* **121,** 1099–1125.

——, and ——, 1993b: The causes of severe convective outbreaks in Alberta. Part II: Conceptual and statistical analysis. *Mon. Wea. Rev.,* **121,** 1126–1133.

——, G. W. Reuter, and M. K. Yau, 1998: The episodic occurrence of hail in central Alberta and the Highveld of South Africa. *Atmos.–Ocean,* **36,** 169–178.

Thompson, R. L., R. Edwards, J. A. Hart, K. L. Elmore, and P. Markowski, 2003: Close proximity soundings within supercell environments obtained from the Rapid Update Cycle. *Wea. Forecasting,* **18,** 1243–1261.

Turcotte, V., and D. Vigneux, 1987: Severe thunderstorms and hail forecasting using derived parameters from standard RAOBS data. Preprints, *Second Workshop on Operational Meteorology,* Halifax, NS, Canada, Atmospheric Environment Service/Canadian Meteorological and Oceanographic Society, 142–153.

Weisman, M. L., and J. B. Klemp, 1982: The dependence of numerically simulated convective storms on vertical wind shear and buoyancy. *Mon. Wea. Rev.,* **110,** 504–520.

——, and ——, 1986: Characteristics of isolated storms. *Mesoscale Meteorology and Forecasting,* P. S. Ray, Ed., Amer. Meteor. Soc., 331–357.